Comparative study of Al_2O_3-YAG:Ce composite ceramic and single crystal YAG:Ce phosphors for high-power laser lighting

Xu, Jian; Yang, Yang; Guo, Ziquan; Corell, Dennis Dan; Du, Baoli; Liu, Bingguo; Ji, Haipeng; Dam-Hansen, Carsten; Jensen, Ole B.

Published in:
Ceramics International

Link to article, DOI:
10.1016/j.ceramint.2020.04.101

Publication date:
2020

Document Version
Peer reviewed version

Comparative Study of Al_2O_3-YAG:Ce Composite Ceramic and Single Crystal YAG:Ce Phosphors for High-Power Laser Lighting

Jian Xu[a,b,*], Yang Yang[a], Ziquan Guo[c], Dennis Dan Corell[b], Baoli Du[a], Bingguo Liu[a], Haipeng Ji[d,*], Carsten Dam-Hansen[b], Ole B Jensen[b]

[a] Lab of New Energy Materials and Devices, School of Physics and Electronic Information, Henan Polytechnic University, Jiaozuo 454000, China

[b] Diode Lasers and LED Systems Group, Department of Photonics Engineering, Technical University of Denmark, Roskilde 4000, Denmark

[c] Fujian Engineering Research Center for Solid-State Lighting, Department of Electronic Science, Xiamen University, Xiamen 361005, China

[d] School of Materials Science and Engineering, Zhengzhou University, Zhengzhou 450001, China

(Declaration of interest: none)

ABSTRACT

Recent studies revealed that both the Al_2O_3-$Y_3Al_5O_{12}$:Ce (YAG:Ce) composite ceramic (YAG-CC) and single crystalline YAG:Ce (YAG-SC) possess very high luminescence-saturation thresholds (LSTs), which makes them promising for laser lighting applications. The present study is aimed to conduct a comparative investigation between YAG-CC and YAG-SC on aspects of the laser-pumped luminescence and the associated thermal behavior. The colorimetric and photometric properties (e.g. luminous flux/efficacy, correlated color temperature, and color rendering index) were investigated systematically, by conducting the measurements using a custom-built sphere-spectroradiometer system in the transmission mode. It was found that YAG-SC has a superior LST and it could maintain a high luminous efficacy (106 lm/W) under the irradiation of a 15.33 W blue laser, while the YAG-CC saturated at around 7.76 W. Moreover, by combining the thermal imaging data with the spectral

variation of the YAG-CC, novel experimental insights into the origin of luminescence saturation were revealed and proposed as the "thermally-induced absorption saturation".

KEYWORDS: Laser lighting; YAG:Ce; Composite ceramic; Single crystal; Luminescence saturation

1. INTRODUCTION

Since the invention of efficient blue light-emitting diodes (LEDs) in 1993, a revolution in lighting technology has been underway, which saw conventional lighting-devices (incandescent, fluorescent, high-intensity-discharge lamps, etc.) being rapidly replaced by LEDs [1]. One of the LEDs' biggest advantages is its high energy-efficiency, which enables a substantial reduction in greenhouse gas emission [2]. However, this high energy-efficiency can only be achieved at very low driving-power because a non-thermal "efficiency droop", that occurs in LEDs at higher input currents [3-5]. Up to now, the origin of the "efficiency droop" has remained unclear, and no effective solution was available.

In comparison, laser diodes (LDs) can maintain relatively high energy-efficiency even at quite high current-densities [3-6]. Thus, LD-based lighting devices are promising contenders for high-brightness and high-luminance applications. Similar to the phosphor-converted white-LEDs (pc-wLEDs), the most popular approach to generate white light for a LD system is to combine the pumping source (i.e., blue LD) with phosphor(s) [7-11]. However, phosphors in pc-wLDs face an entirely new challenge, known as "luminescence saturation", due to the more intense irradiation of LDs than LEDs [12-15]. It occurs when the laser irradiation reaches a certain value, at which point the luminescence intensity of the phosphor will not increase anymore, or even decreases (often substantially). For this reason, phosphors for pc-wLDs need to possess a high luminescence saturation threshold (LST) to withstand the high-level irradiation, and thus enable high-brightness and high-luminance [11, 16-19].

In pc-wLDs, cerium-doped yttrium aluminum garnet ($Y_3Al_5O_{12}$:Ce, YAG:Ce) is inherited as a

candidate of yellow-emitting phosphor because of its broad emission band, suitable absorption/emission wavelength, fast luminescence decay, high thermal conductivity, and relatively weak thermal quenching of luminescence [6, 9, 10, 17, 20-22]. Many studies have been performed to improve the LST of YAG:Ce-based phosphors. The published references results reveal that both Al_2O_3-YAG:Ce composite ceramic (YAG-CC) and single crystalline YAG:Ce (YAG-SC) possess a superior LST than other types of YAG:Ce phosphors, for example, YAG phosphor-in-glass, and phosphor layer [12, 17, 22-24]. Li et al. reported a YAG-CC that showed no sign of luminescence saturation pumped by a blue laser with a power density 50 W/mm^2 [8]. Cozzan et al. reported a YAG-CC that showed a LST over 7 W [10]. For the YAG-SC phosphor, Xu et al. found that the YAG-SC has a remarkably high LST that there is no sign of luminescence intensity/luminous flux decline even when the driven laser power density reaches 360 W/mm^2 [9].

In spite of the impressive LST of YAG-CC and YAG-SC, several challenges remain to be approached. Firstly, due to limitations of the experimental conditions (e.g., the underpowering of the driven laser), the exact LSTs of YAG-CC and YAG-SC remain undetermined [8, 10]. Secondly, some researchers use laser-power-dependent emission-intensity or flux to evaluate the saturation properties, while others use laser-power-density-dependent data. These non-uniform characterization methods make it difficult for accurate comparisons (between YAG-CC and YAG-SC). Thirdly, because of the lack of the observation at luminescence saturation state, the underlying mechanism responsible for luminescence saturation in YAG:Ce remains to be clarified. The luminescence saturation has been observed in YAG:Ce based phosphor-in-glass (PiG) [17, 25]. However, the glass matrix could introduce many uncertainties (e.g., crystallization, melting and fracturing of the glass during laser irradiation), which significantly hindered the exploration of the origin of the luminescence saturation.

Lastly, both the YAG-CC and YAG-SC are transparent, or translucent, which enables them to be used in transmission mode. However, most of the aforementioned studies were performed in reflection mode.

In light of the fundamental and technical difficulties mentioned above, a comparative study between YAG-CC and YAG-SC was conducted. By employing a 38 W laser-module in a custom-built sphere-spectroradiometer, the colorimetric and photometric properties (e.g., luminous flux/efficacy, and correlated color temperature) of YAG-CC and YAG-SC were systematically investigated. It was found that the YAG-SC is superior to the YAG-CC in a number of laser-lighting-related aspects (including the LST, luminous efficacy, and robustness). Furthermore, by observing and analyzing the thermal and optical properties of the YAG-CC for the luminescence saturation state, novel experimental insights into the origin of luminescence saturation, termed as "thermally-induced absorption-saturation", were proposed and developed.

2. Experiments

The YAG-SC samples are commercially available (Hefei Kejing Materials Technilogy Co., Ltd) with purity exceeding 99.999%, Ce concentration of 0.2 mol%, thickness of 0.5 mm, and luminescence lifetime of 70 ns. The YAG-CC was synthesized via spark plasma sintering (Sumitomo, SPS-3.20-mkII). Commercial YAG:Ce powder (Hangzhouyinghe CO., LTD, YH552M) and α-Al_2O_3 (99.99%, Aladdin, 5-6 μm) were mixed at a weight ratio of 1:1. A graphite sheet with a thickness of 0.3 mm was rolled into a tube and attached to the internal surface of a graphite die (Φ = 12 mm). Then, a boron nitride (BN) layer was sprayed on the graphite sheet for lubrication and insulation. Next, 1.2 g of the mixed powder was loaded into the die and sintered at 1450 °C for 30 min with a uniaxial force of 10 kN. After the heat treatment, the sample was machined and polished to a thickness of around 150 μm to

achieve an equivalent correlated color temperature (CCT) with that of the YAG-SC (about 4600 K). The YAG-SC and YAG-CC possess similar in-line transmittance which are ~12% and ~10% (at 550 nm), respectively.

The surface morphology was observed using a scanning electron microscope (SEM, TM-3030 plus, Hitachi). Both the YAG-CC and YAG-SC phosphors were glued to a heat sink with a hole ($\Phi \approx 3$ mm) in the center to let light pass through. A schematic of the high-power laser module and the sphere-spectroradiometer system is shown in Figure 1. The high-power laser module consists of 8 (i.e., 2 × 4 array) blue LDs (NUBM-08, 4.75 W × 8, $\lambda_{em} \approx 450$ nm, Nichia). The laser beam was collimated and focused by 2 achromatic lenses (lens-1: diameter = 50 mm, focal length = 250 mm; lens-2: diameter = 25 mm, focal length = 50 mm) with a spot area of around 2 mm^2. The sphere-spectroradiometer system consists of a fiber-coupled integrating sphere (Labsphere, 1-meter diameter) with an array spectrometer (Instrument Systems, CAS-140-CT-151). It is used in forward flux or 2π geometry using the 50 mm input port. The photoluminescence spectra and the quantum efficiency (QE) were measured with a custom-built sphere-spectroradiometer (HORIBA, Fluorolog-3) equipped with an integrating sphere with a diameter of 30 cm. The thermal images were captured with an infrared camera (FLIR, A655sc). The light distribution was measured using a near-field goniophotometer (Technoteam, RiGo-801).

3. Results and Discussion

The laser-pumped emission spectra (Figure 2 a and b) as well as the luminous flux (Figure 2 c) and the luminous efficacy (Figure 2 d) of the samples are shown in Figure 2. All emission spectra consist of a sharp peak located at around 450 nm from the blue LD module, and a broad emission band at 475-800 nm originating from the Ce^{3+} $5d \rightarrow 4f$ luminescence of YAG:Ce [20, 26]. In Figure 2 (a), the emission intensity of the YAG-SC increases monotonously with the increase of laser power from 0.15

W to 15.33 W, while a sudden plunge occurs at 16.80 W. In contrast, the sudden drop in case of the YAG-CC appears at 9.30 W, indicating a lower LST during laser irradiation in YAG-CC. As seen from Figure 2 (c), a high luminous flux of 1618 lm was achieved using the YAG-SC phosphor. In contrast, the device using the YAG-CC can only reach a maximum luminous flux of 631 lm. Considering the almost identical internal quantum efficiency (IQE, both around 90%) and CCT (about 4600 K) of YAG-CC and YAG-SC, the luminous efficacies of devices using both phosphors should be comparable. However, the luminous efficacy of YAG-SC (121 lm/W at 0.15 W) is substantially higher than that of YAG-CC (93 lm/W at 0.15 W). The underlying reasons for this unexpected discrepancy are going to be discussed in the next section. The luminous efficacies using both phosphors are expected to be significantly improved if a blue-passing-yellow-reflecting (BPYR) layer is used.

The variations of the CCT of the laser pumped devices are shown in Figure 3. Prior to the occurrence of the saturation, both materials showed a CCT of around 4600 K, which is suitable for general lighting applications. The CCTs variations are consistent with the photometric results shown in Figure 2, where YAG-SC appears to be obviously more robust than YAG-CC. In general, the blue/yellow ratio has a primary weight with regard to CCT. Thus, the saturation of a phosphor could result in an extremely high CCT value (> 10000 K) for the light source. For YAG-SC, a remarkable fluctuation in the CCT can be observed between the initial laser power and 13.85 W. In this laser power range, the change of the blue/yellow ratio is not significant. The emission spectra of the YAG-SC reveal a clear redshift (527 nm → 540 nm) which is caused by the increasing temperature that decreases the CCT [28]. Thus, a fluctuation of CCT was observed in YAG-SC.

For safe operation and to maximize the color quality, a homogeneous mix of laser emission and phosphor emission is desired for a pc-wLD. Owing to the scattering properties of the composite

ceramic, the YAG-CC can effectively diffuse the incident blue laser light, which mixes well with the yellow emission from the YAG-CC, and generate uniform white light. The lighting effect is shown in Figure 4 (a) from which the uniformity in color mixing can be distinguished. This result is consistent with the previous study, which was conducted in the reflection mode. The lighting effect of YAG-SC, however, see Figure 4 (b), shows a clear transmitted laser spot, which suggests poor color uniformity. It is worth noting that the surface of YAG-SC is unpolished and its surface SEM image is shown in Figure 4 (c). The color distribution was measured using the setup near-field goniophotometer schematically shown in Figure 4 (d) where the detector is a camera equipped with a filter wheel. In Figure 4 (e and f), the detector was equipped with a blue filter, therefore, only light coming from the laser was collected. It is noteworthy that the yellow light distribution (from the phosphor) is naturally uniform, thus the (blue) laser light distribution plays decisive role for the color uniformity of the light source. The results in Figure 4 (e and f) confirmed that the blue laser light for YAG-SC failed to be scattered effectively and its spatial distribution was much narrower than that of the blue laser light for YAG-CC. A diffusion coating layer may solve this problem.

Both the YAG-SC and YAG-CC show a nearly identical CCT and IQE, which should also possess similar luminous efficacies. However, the measurements indicate that YAG-SC (121 lm/W at 0.15 W) has a much higher (around 29%) luminous efficacy than YAG-CC (93 lm/W at 0.15 W). Most likely, this is due to the scattering losses in YAG-CC. Compared to the nearly perfect configuration and crystal structure of YAG-SC, there is a clear mismatch between the refractive indices of the YAG:Ce particles and the α-Al_2O_3 matrix in YAG-CC. This means that both the incident blue laser and the emitted light (from the phosphor) are highly scattered. Moderate scattering can improve the external QE of a phosphor by facilitating blue-light extraction. This also explains the fact that the YAG-CC can reach a

CCT equivalent to the YAG-SC but with much thinner the thickness. However, the scattering of the emitted light from the phosphor inevitably increases the re-absorption probability, which consequently causes more energy loss and a lower luminous efficacy.

The heat dissipation capability of a phosphor is critical to LST. Due to the very high thermal conductivity (> 35 W/m K) of the α-Al_2O_3 matrix, the YAG-CC shows superior thermal conductivity (~18 W/m K) compared to YAG-SC (~10 W/m K). On the other hand, YAG-SC has a substantially higher LST (around 15.33 W) than YAG-CC (7.76 W). This unexpected result is probably due to the following two reasons. One is that YAG-SC shows smaller thermal-quenching than YAG-CC. For example, at 200 °C, the intensity drop (with respect to the intensity at room temperature) for YAG-SC is about 3%, while the intensity drop for YAG-CC reaches up to about 9%. With increasing operating-temperature, larger thermal-quenching decreases the IQE. This can further increase the conversion loss, which ultimately reduces the LST. Another reason is related to the average distance between the Ce^{3+} in the YAG:Ce-based phosphors. When a laser beam irradiates YAG:Ce, each Ce^{3+} can be regarded as a heat source. This is because the inevitable energy loss during the photoluminescence process (Stokes loss and the conversion loss) is ultimately converted to thermal energy, which leads to self-heating. A schematic of the microstructures of the studied phosphors is shown in Figure 5. In YAG-SC, the Ce^{3+} doping concentration is low (0.2 mol%), and its distribution is uniform. In contrast, the YAG:Ce powder, which is used in YAG-CC, has a much higher doping concentration (2 mol%). Furthermore, there is no Ce^{3+} in the matrix phase, which indicates that the actual average distance between Ce^{3+} in the YAG:CC is significantly shorter than in YAG-SC. Therefore, the thermal coupling between Ce^{3+} is much stronger in YAG-CC. In addition, a shorter average distance between the activators probably also facilitate the excited state interaction, which also reduces the LST.

Generally, the $5d_1$ to $4f$ transition in Ce^{3+} is both parity- and spin-allowed and shows a fast decay - in the range of 40-70 ns. The fast relaxation from the Ce^{3+} $5d_1$ excited state to the ground state ($^2F_{5/2}$, $^2F_{7/2}$) shows an advantage by avoiding the "excited state absorption", which suggests a very high saturation threshold at high laser-power density [9, 20, 26, 27]. It was an outcome of our previous study that YAG-SC does not show luminescence saturation even when the laser power density reaches 360 W/mm^2 [9]. In that case, the total laser power was relatively low (< 4 W). In this study, clear luminescence saturation occurred at high total power/low power density irradiation with the laser. As shown in Figure 6 (a), when the laser power increases to 9.30 W from 7.76 W, the surface temperature of the YAG-CC increases to 660 °C from 160 °C. A higher laser power produces more conversion loss, which results in more vigorous "self-heating" and higher operating temperatures. For YAG:Ce-based phosphors, the optical/absorption saturation is generally not considered the main reason for luminescence saturation. Surprisingly, the transmitted laser light (in the integrating sphere) shows a disproportionate increase: the spectral intensity at 9.30 W was 2 times greater than at 7.76 W. High transmittance means low absorption, which suggests the occurrence of optical/absorption saturation. It has been shown that the photoionization of the $5d^1$ electron (of Ce^{3+}) into the conduction band of the YAG host when temperature reaches 300 °C, quenches the luminescence and prolongs the time needed for the Ce^{3+} ions to return to the ground state [26]. This results in a considerable increase of the luminescence decay time for Ce^{3+}, which leads to depletion of Ce^{3+} available for being readily pumped into the excited state, and ultimately leads to absorption saturation in YAG:Ce. Thus, the luminescence saturation in YAG:Ce is probably not only caused by thermal quenching, but also related to thermally-induced absorption saturation.

4. Conclusions

In summary, we comparatively investigated the blue laser-pumped lighting properties of YAG-CC and YAG-SC. Using a custom-built sphere-spectroradiometer, both phosphors were investigated in transmissive mode. It was found that the YAG-SC has a much higher luminous efficacy (121 lm/W) and higher luminescence-saturation threshold (> 15.33 W) than these of the YAG-CC. When pumped with a 15.33 W blue laser, the YAG-SC-based pc-wLD reached a very high luminous flux of 1618 lm, while the pc-wLD, based on the YAG-CC, shows very high light homogeneity, significantly better than for YAG-SC, due to intense scattering by the phase/crystal boundaries. In addition, saturated absorption was observed in YAG:Ce, and was correlated to the prolonged decay-time of Ce^{3+} aroused by the photoionization of $5d^1$ electron (of Ce^{3+}) into the conduction band of the YAG host and depletion of Ce^{3+} in ground state. Thus, the thermally-induced absorption saturation is probably one of the reasons causing the luminescence saturation.

Acknowledgements

This work was supported by National Natural Science Foundation of China (NSFC 51772076 and 51802083), Danish Energy Technology Development and Demonstration program (EUDP 64017-0588), Natural Science Foundation of Fujian Province (2019J05022), Scientific Research Foundation of Henan Polytechnic University (B2017-58 and T2017-2) and Postdoctoral Research Sponsorship in Henan Province (19030025). JX thanks the China Scholarship Council for the financial support for his stay at the Diode Lasers and LED Systems Group (DTU Fotonik) to carry out this work.

References

[1] E.F. Schubert, J.K. Kim, Solid-State Light Sources Getting Smart, Science, 308 (2005) 1274.

[2] S. Pimputkar, J.S. Speck, S.P. DenBaars, S. Nakamura, Prospects for LED lighting, Nature Photonics, 3 (2009) 180.

[3] J.J. Wierer, J.Y. Tsao, D.S. Sizov, Comparison between blue lasers and light-emitting diodes for future solid-state lighting, Laser & Photonics Reviews, 7 (2013) 963-993.

[4] J. Piprek, Comparative efficiency analysis of GaN-based light-emitting diodes and laser diodes, Applied Physics Letters, 109 (2016) 021104.

[5] Y.C. Shen, G.O. Mueller, S. Watanabe, N.F. Gardner, A. Munkholm, M.R. Krames, Auger recombination in InGaN measured by photoluminescence, Applied Physics Letters, 91 (2007) 141101.

[6] S. Li, L. Wang, N. Hirosaki, R.J. Xie, Color Conversion Materials for High-Brightness Laser-Driven Solid-State Lighting, Laser & Photonics Reviews, 12 (2018) 1800173.

[7] J. Xu, J. Wang, Y. Gong, X. Ruan, Z. Liu, B. Hu, B. Liu, H. Li, X. Wang, B. Du, Investigation of an LuAG:Ce translucent ceramic synthesized via spark plasma sintering: Towards a facile synthetic route, robust thermal performance, and high-power solid state laser lighting, Journal of the European Ceramic Society, 38 (2018) 343-347.

[8] S. Li, Q. Zhu, D. Tang, X. Liu, G. Ouyang, L. Cao, N. Hirosaki, T. Nishimura, Z. Huang, R. J. Xie, Al_2O_3–YAG:Ce composite phosphor ceramic: a thermally robust and efficient color converter for solid state laser lighting, Journal of Materials Chemistry C, 4 (2016) 8648-8654.

[9] J. Xu, A. Thorseth, C. Xu, A. Krasnoshchoka, M. Rosendal, C. Dam-Hansen, B. Du, Y. Gong, O.B. Jensen, Investigation of laser-induced luminescence saturation in a single-crystal YAG:Ce phosphor: Towards unique architecture, high saturation threshold, and high-brightness laser-driven white lighting,

Journal of Luminescence, 212 (2019) 279-285.

[10] C. Cozzan, G. Lheureux, N. O'Dea, E.E. Levin, J. Graser, T.D. Sparks, S. Nakamura, S.P. DenBaars, C. Weisbuch, R. Seshadri, Stable, Heat-Conducting Phosphor Composites for High-Power Laser Lighting, ACS applied materials & interfaces, 10 (2018) 5673-5681.

[11] Y. Yuan, D. Wang, B. Zhou, S. Feng, M. Sun, S. Zhang, W. Gao, Y. Bi, H. Qin, High luminous fluorescence generation using Ce:YAG transparent ceramic excited by blue laser diode, Optical Materials Express, 8 (2018) 2760.

[12] Q.Q. Zhu, X.J. Wang, L. Wang, N. Hirosaki, T. Nishimura, Z.F. Tian, Q. Li, Y.Z. Xu, X. Xu, R.J. Xie, β-Sialon:Eu phosphor-in-glass: a robust green color converter for high power blue laser lighting, Journal of Materials Chemistry C, 3 (2015) 10761-10766.

[13] A. Krasnoshchoka, A. Thorseth, C. Dam-Hansen, D.D. Corell, P.M. Petersen, O.B. Jensen, Investigation of Saturation Effects in Ceramic Phosphors for Laser Lighting, Materials, 10 (2017) 1407.

[14] T. Jansen, D. Böhnisch, T. Jüstel, On the Photoluminescence Linearity of Eu2+Based LED Phosphors upon High Excitation Density, ECS Journal of Solid State Science and Technology, 5 (2016) R91-R97.

[15] S. Li, Q. Zhu, L. Wang, D. Tang, Y. Cho, X. Liu, N. Hirosaki, T. Nishimura, T. Sekiguchi, Z. Huang, R.J. Xie, CaAlSiN3:Eu^{2+} translucent ceramic: a promising robust and efficient red color converter for solid state laser displays and lighting, Journal of Materials Chemistry C, 4 (2016) 8197-8205.

[16] L. Wang, R.-J. Xie, T. Suehiro, T. Takeda, N. Hirosaki, Down-Conversion Nitride Materials for Solid State Lighting: Recent Advances and Perspectives, Chemical reviews, 118 (2018) 1951-2009.

[17] P. Zheng, S. Li, L. Wang, T.L. Zhou, S. You, T. Takeda, N. Hirosaki, R.J. Xie, Unique Color Converter Architecture Enabling Phosphor-in-Glass (PiG) Films Suitable for High-Power and High-Luminance Laser-Driven White Lighting, ACS applied materials & interfaces, 10 (2018) 14930-14940.

[18] L. Kang, S. Yun, F. Jia, C. Price, Y. Gong, J. Huang, N. Copner, C. Hui, L. Yang, S. Chen, Low Etendue Yellow-Green Solid-State Light Generation by Laser-pumped LuAG:Ce Ceramic, IEEE Photonics Technology Letters, PP (2018) 939-942.

[19] N. Trivellin, M. Yushchenko, M. Buffolo, C. De Santi, M. Meneghini, G. Meneghesso, E. Zanoni, Laser-Based Lighting: Experimental Analysis and Perspectives, Materials, 10 (2017) 1166.

[20] V. Bachmann, C. Ronda, A. Meijerink, Temperature Quenching of Yellow Ce^{3+} Luminescence in YAG:Ce, Chemistry of Materials, 21 (2009) 2077-2084.

[21] J. Park, S. Cho, H. Kwon, Aluminum-ceramic composites for thermal management in energy-conversion systems, Scientific reports, 8 (2018) 17852.

[22] J. Xu, B. Liu, Z. Liu, Y. Gong, B. Hu, J. Wang, H. Li, X. Wang, B. Du, Design of laser-driven SiO_2-YAG:Ce composite thick film: Facile synthesis, robust thermal performance, and application in solid-state laser lighting, Optical Materials, 75 (2018) 508-512.

[23] X. Zhang, J. Yu, J. Wang, B. Lei, Y. Liu, Y. Cho, R.J. Xie, H.W. Zhang, Y. Li, Z. Tian, Y. Li, Q. Su, All-Inorganic Light Convertor Based on Phosphor-in-Glass Engineering for Next-Generation Modular High-Brightness White LEDs/LDs, ACS Photonics, 4 (2017) 986-995.

[24] H. Lin, T. Hu, Y. Cheng, M. Chen, Y. Wang, Glass Ceramic Phosphors: Towards Long-Lifetime High-Power White Light-Emitting-Diode Applications-A Review, Laser & Photonics Reviews, 12 (2018) 1700344.

[25] X. Zhang, S. Si, J. Yu, Z. Wang, J. Wang, Improving the luminous efficacy and the resistance to

blue laser irradiation of phosphor-in-glass based solid state laser lighting through employing dual-functional sapphire plate, Journal of Materials Chemistry C, 7 (2019) 354-361.

[26] J. Ueda, P. Dorenbos, A.J.J. Bos, A. Meijerink, S. Tanabe, Insight into the Thermal Quenching Mechanism for $Y_3Al_5O_{12}:Ce^{3+}$ through Thermoluminescence Excitation Spectroscopy, The Journal of Physical Chemistry C, 119 (2015) 25003-25008.

[27] D.S. Hamilton, S.K. Gayen, G.J. Pogatshnik, R.D. Ghen, W.J. Miniscalco, Optical-absorption and photoionization measurements from the excited states of $Ce^{3+}:Y_3Al_5O_{12}$, Phys Rev B Condens Matter, 39 (1989) 8807-8815.

[28] S. Yan, On the origin of temperature dependence of the emission maxima of $Eu^{2+}$and Ce^{3+}- activated phosphors, Optical Materials, 79 (2018) 172-185.

Figure Captions

Figure 1. Schematic of the high-power laser module and the sphere-spectroradiometer system.

Figure 2. Emission spectra of the laser pumped devices using the YAG-SC (a) and YAG-CC (b) phosphors with varying laser power (from 0.15 W to the respective saturation power). (c) and (d) show the evolution of the luminous flux and the luminous efficacy, respectively.

Figure 3. CCT variations of the phosphors for increasing laser power.

Figure 4. The lighting effects the of (a) YAG-CC and (b) YAG-SC; insets are the corresponding sample images; (c) the surface SEM image of the YAG-SC; (d) Schematic of the setup to measure the light distribution of the transmission-mode light source; The laser light distributions (e and f) of the white light sources that are based on the YAG-SC and YAG-CC, respectively.

Figure 5. Schematic of the microstructure of the investigated phosphors.

Figure 6 (a) Zoomed spectra for the blue laser near the saturation state of YAG-CC. The shown powers (5.90 W, 7.76 W and 9.30 W) are the output powers of the laser module, which were obtained before hitting the phosphor. The shown spectra are for the transmitted laser light and were obtained using the sphere-spectroradiometer. The inserts represent the corresponding thermal distribution images. (b) Vacuum-referred binding energy diagram of YAG:Ce^{3+} showing the mechanism of thermally-induced absorption saturation at high-power laser irradiation.

Figures

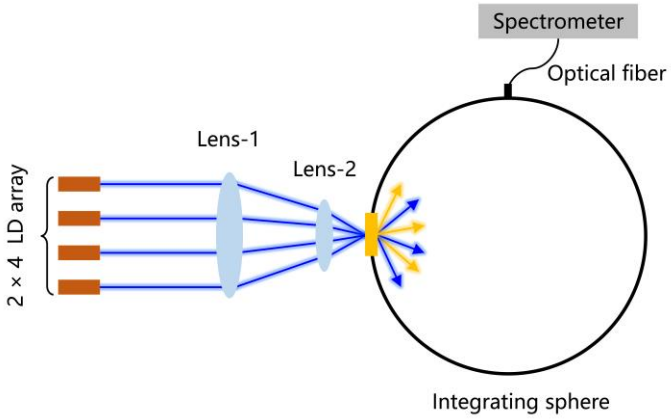

Figure 1

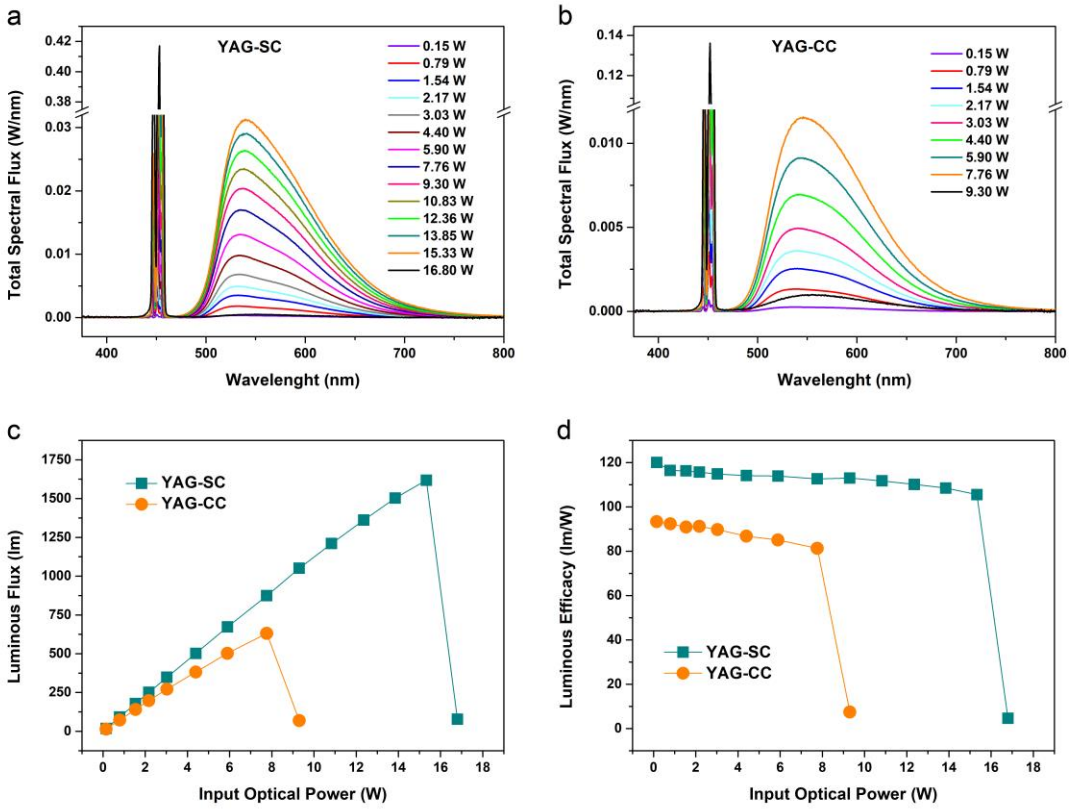

Figure 2

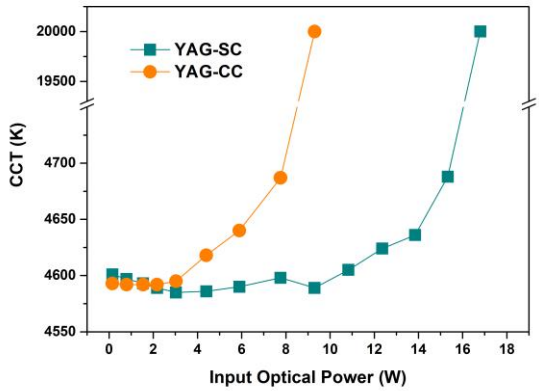

Figure 3

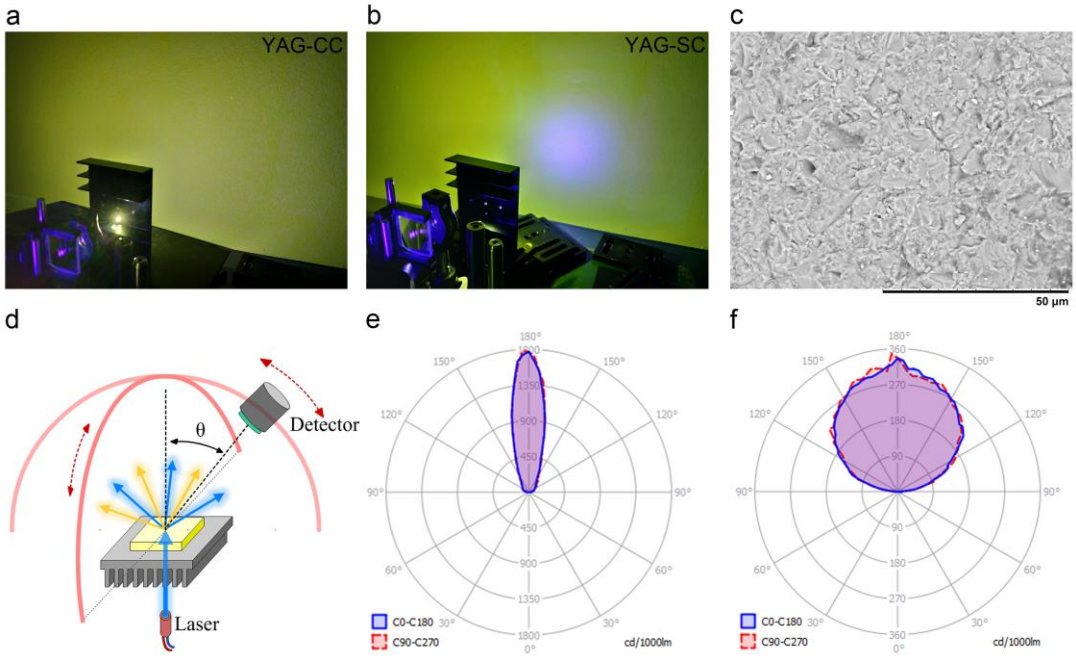

Figure 4

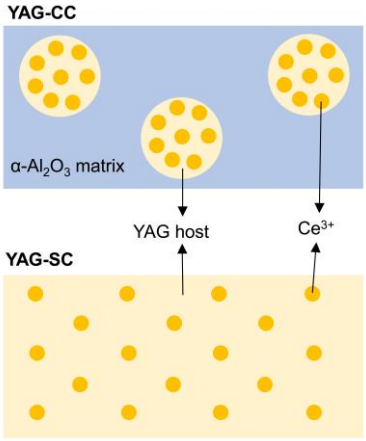

Figure 5

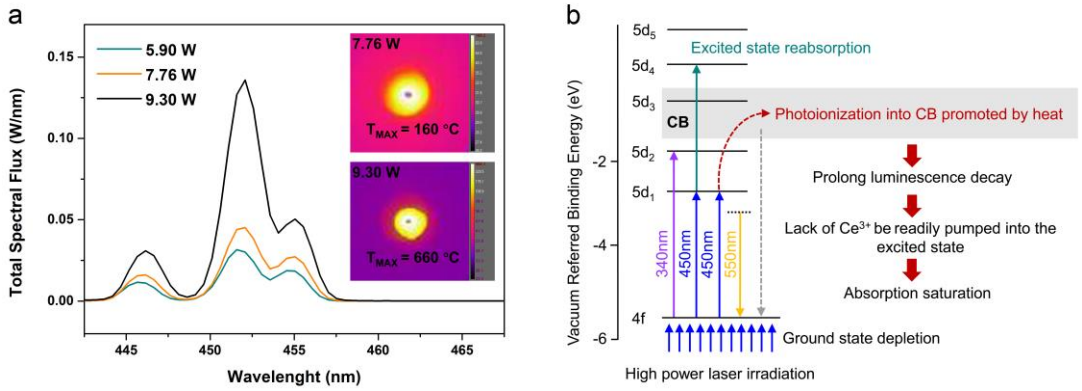
a
5.90 W
7.76 W
9.30 W
7.76 W
T_MAX = 160 °C
9.30 W
T_MAX = 660 °C
Total Spectral Flux (W/nm)
0.15
0.10
0.05
0.00
445
450
455
460
465
Wavelenght (nm)
b
5d5
5d4
5d3
CB
5d2
5d1
4f
Excited state reabsorption
Photoionization into CB promoted by heat
Prolong luminescence decay
Lack of Ce3+ be readily pumped into the excited state
Absorption saturation
Ground state depletion
340nm
450nm
450nm
550nm
Vacuum Referred Binding Energy (eV)
-2
-4
-6
High power laser irradiation

Figure 6